International Symposium
On Turbulence and Shear Flow
Phenomena (TSFP-8)
August 28 - 30, 2013 Poitiers, France

DNS OF TURBULENT DRAG REDUCTION BY SPANWISE WALL FORCING: THE REYNOLDS NUMBER EFFECT

Yongmann M. Chung
School of Engineering and Centre for Scientific Computing,
University of Warwick
Coventry, CV4 7AL, U.K.
Y.M.Chung@warwick.ac.uk

Edward Hurst, Q. Oliver Yang
School of Engineering and Centre for Scientific Computing,
University of Warwick
Coventry, CV4 7AL, U.K.

ABSTRACT

The Reynolds effect of streamwise travelling waves of spanwise wall velocity on turbulent channel flow has been investigated using DNS. Simulations with various control parameters are performed at four Reynolds numbers, corresponding to $Re_\tau = 200, 400, 800$ and 1600. As the Reynolds number is increased, it is found that the intensity of both the drag reduction and drag increase is reduced, and this change does not scale universally. The value of the optimal forcing parameters changes with Reynolds number, even in wall units. Consequently, the drag reduction deteriorates quickly with Reynolds number when the parameters used are close to optimal at a lower Re number.

INTRODUCTION

With high levels of energy consumption and CO_2 emissions associated with various methods of transportation, there is a huge requirement for ways to reduce frictional drag. In particular, the aircraft industry is seeking to increase fuel efficiency by reducing the skin friction drag during cruise, to meet the ACARE 2020 (Advisory Council for Aeronautics Research in Europe) target of a 50% reduction in emissions by 2020 (Bieler et al., 2006; Chung and Talha, 2011). Wall forcing has been shown to attain a drag reduction (DR) as high as 40% at a Reynolds number of $Re_\tau = 200$ (Jung et al., 1992; Karniadakis and Choi, 2003; Quadrio and Ricco, 2004). The amount of drag reduction can be defined as $\mathcal{DR} = \left(1 - \frac{C_f}{C_{f,0}}\right) \times 100(\%)$.

Streamwise travelling waves of spanwise wall velocity have been studied by applying the following forcing at the wall:

$$w_w(x,t) = W_m \sin\left(\kappa_x x - \omega t\right),$$

where W_m is the maximum wall velocity, κ_x is the streamwise wavenumber and ω is the oscillation frequency. When $\kappa_x = 0$, the forcing becomes the purely temporal wall oscillation case (Jung et al., 1992; Quadrio and Ricco, 2004), and the $\omega = 0$ case specifies the purely spatial stationary wave (Viotti et al., 2009). The travelling wave can, therefore, be considered to be a spatial wave, with wavenumber κ_x, travelling at velocity $c = \omega/\kappa_x$. At $Re_\tau = 200$ it has been shown (Quadrio et al., 2009) that the maximum drag reduction was achieved by a forward travelling wave ($c > 0$). However, forward travelling waves close to a specific phase speed ($c \approx 0.5$) can actually give a drag increase (DI).

Re Number Effect

For high Reynolds number situations, an understanding of the Reynolds number effect is crucial, as a knowledge of the drag reduction achievable gives an important insight into the applicability of the control method. The effect of Reynolds number on the efficacy of flow control has been observed for the opposition control (Iwamoto et al., 2002; Chang et al., 2002). However, the majority of previous study on spanwise oscillation has been confined to lower Re numbers, $Re_\tau = 200$ and below; only few simulations have been performed at higher Reynolds numbers. Ricco and Quadrio (2008) performed three wall oscillation simulations at $Re_\tau = 400$, with $W_m^+ = 12$ and $T^+ = 30$, 125 and 200, and a decrease in the drag reduction was shown. More recently, Touber and Leschziner (2012) studied wall oscillation at $Re_\tau = 500$ and 1000. The Reynolds number effect is also mentioned by Quadrio et al. (2009) for travelling waves. Using the optimal parameters from the $Re_\tau = 200$ simulations, they reported that the maximum $\mathcal{DR}$ depended weakly on the Re number; the $\mathcal{DR}$ reduced from 48% to 42% as Re increased to $Re_\tau = 400$.

An insight into the effect of Reynolds number on spanwise wall forcing has been given recently by Quadrio and Gatti (2012), with some similarities to the current study (Hurst and Chung, 2012a,b). Understanding the effect of Reynolds number on the drag reduction achieved by the control strategy is extremely useful and can help ascertain the applicability of the forcing to high Reynolds number situations. In order to fully understand the Re number scaling for spanwise wall forcing method, it is preferable to study a multitude of forcing parameters at increased Reynolds number, as opposed to the few parameters studied in previous simulations. This is challenging due to the great computational cost of accurate high Reynolds number DNS. The current work seeks to improve current knowledge by expanding the range of parameters studied at $Re_\tau = 400$ and 800, and then extending the limit of the Reynolds number studied as far as $Re_\tau = 1600$.

METHOD

Numerical Procedure

The results presented are generated by a second order finite-volume DNS code (Talha, 2012), based on the fully im-

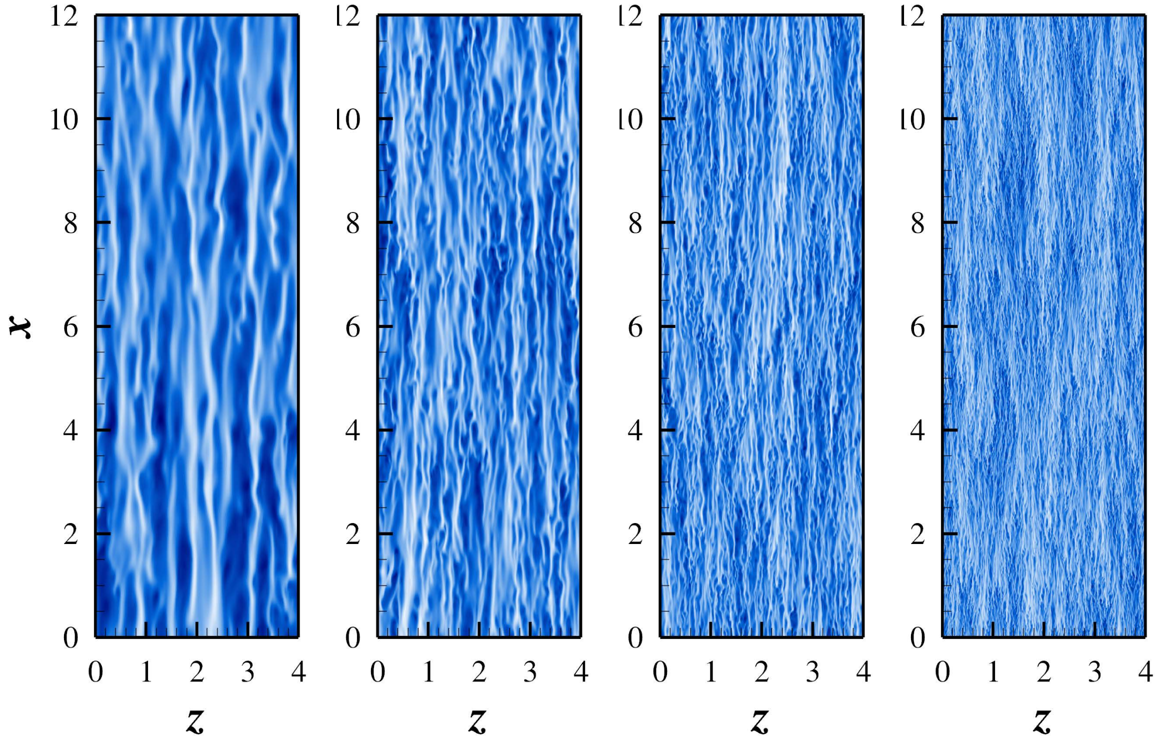

Figure 1: Low-speed streaks at $y^+ = 10$ for no control case for four Re numbers. (a) $Re_\tau = 200$, (b) $Re_\tau = 400$, (c) $Re_\tau = 800$, and (d) $Re_\tau = 1600$.

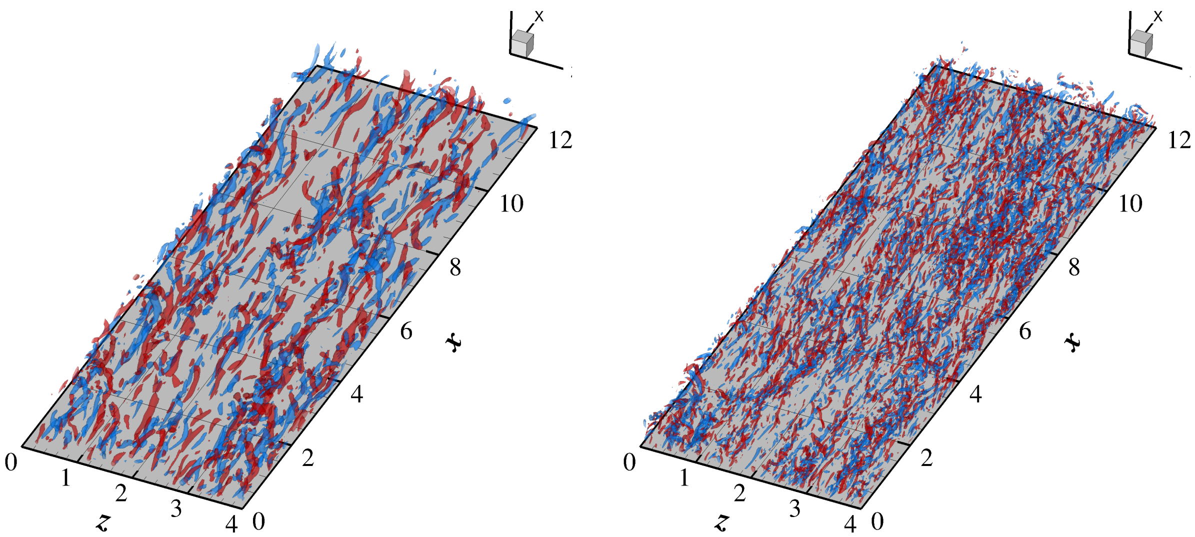

Figure 2: Flow structures (λ_2) for no control case. (a) $Re_\tau = 200$, (b) $Re_\tau = 400$, (c) $Re_\tau = 800$, and (d) $Re_\tau = 1600$.

Re_τ	200	400	800	1600
Re_b	3150	7000	15700	34500
$L_x \times L_y \times L_z$	$16h \times 2h \times 6h$	$16h \times 2h \times 6h$	$12h \times 2h \times 4h$	$12h \times 2h \times 4h$
$N_x \times N_y \times N_z$	$320 \times 140 \times 240$	$640 \times 240 \times 480$	$960 \times 384 \times 640$	$1920 \times 800 \times 1280$
$\Delta x^+, \Delta y^+, \Delta z^+$	$10, 0.4 - 6, 5$	$10, 0.4 - 7.2, 5$	$10, 0.4 - 9.7, 5$	$10, 0.4 - 9.2, 5$

Table 1: Simulation parameters for the four Reynolds numbers studied. Here, h is the channel half-height.

plicit fractional step method proposed by Kim et al. (2002), in which a Crank-Nicolson discretisation is used for both the diffusion and convective terms. When considering parallelisation using MPI, a pencil structure is adopted, dividing the processes into a 2D grid. The code makes use of the 2DECOMP&FFT library developed by Li and Laizet (2010),

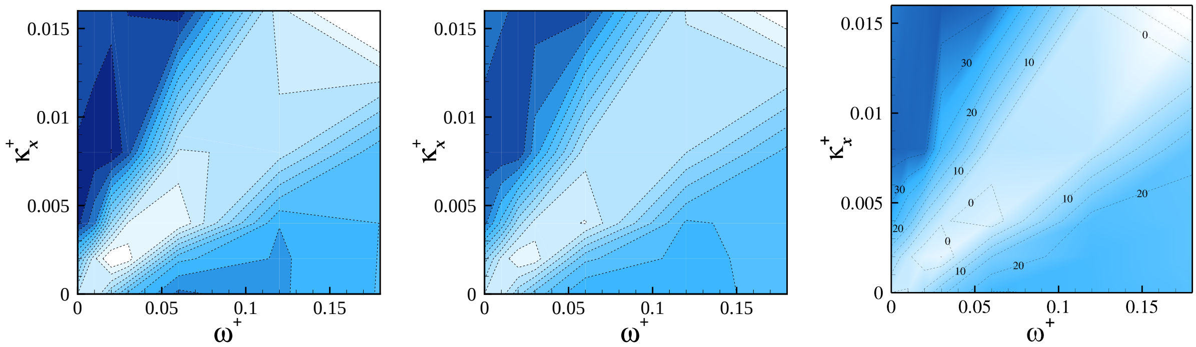

Figure 3: Drag reduction map for the forward travelling waves at (a) $Re_\tau = 200$, (b) $Re_\tau = 400$, and (c) $Re_\tau = 800$. Contour levels are drawn at 5% intervals. The dark blue colour indicates a drag increase, and the light blue indicates a drag reduction.

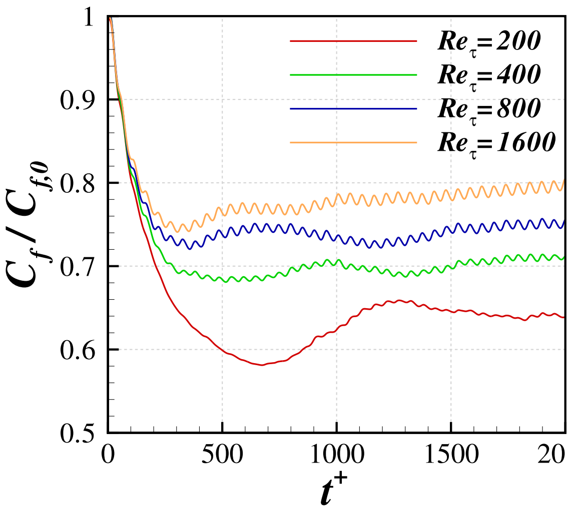

Figure 4: Initial response of skin-friction (normalised by the no control case) at the four Reynolds numbers. The forcing used is the near-optimal wall oscillation case from $Re_\tau = 200$, with $\omega^+ = 0.06$

which performs optimised transpositions when all the data is required in a particular direction. It utilises a set of halo cells for calculations requiring only local data, to reduce the number of necessary transpositions. Parallel I/O is also used to remove the dependency upon writing data and improve efficiency. Simulations with $Re_\tau = 200$, 400 and 800 were performed using a local cluster at Warwick Centre for Scientific Computing (CSC). The higher Reynolds number simulations with $Re_\tau = 1600$ were run on 1024 cores on HECToR (www.hector.ac.uk).

Simulation Parameters

Direct numerical simulations of the turbulent channel flow were performed at four Reynolds numbers $Re_\tau = 200$, 400, 800 and 1600, based on the frictional velocity of the no control case, $u_{\tau 0}$. The simulations were run with a constant mass flow rate. The Reynolds numbers based on the bulk velocity, domain sizes, grid sizes and resolutions are shown in Table 1. Throughout this paper $^+$ represents the wall units based on $u_{\tau 0}$. The domain length is chosen so that the same wall forcing parameters, scaled by wall units, can be studied at each of the Reynolds numbers, due to the requirement of an integer number of waves within the domain. The no control case results compared well with available DNS data from the literature.

The current simulations are restricted to forward travelling waves, corresponding to positive values of ω and κ_x. Using these parameters, the region of maximum drag reduction and the region of drag increase can be investigated. At $Re_\tau = 200$, 400 and 800, simulations are performed with various forcing parameters (ω, κ_x) to produce drag reduction maps (Quadrio et al., 2009). The parameters which achieved maximum $\mathcal{DR}$ for the wall oscillation and stationary wave at $Re_\tau = 800$ were also run at $Re_\tau = 1600$. To the best of the authors' knowledge, this is the highest Re number attempted for flow control DNS.

RESULTS AND DISCUSSION

Uncontrolled Flow

Figure 1 shows the streak patterns of no-control cases for four Re numbers considered. The window size $(12h \times 4h)$ used in the figure is the same for all cases. The low-speed streaks become increasingly smaller with Re number, highlighting the challenges for the high Re number DNS study. The corresponding λ_2 flow structures are shown in Figure 2.

Drag Reduction Map

Figure 3 shows the drag reduction map for $Re_\tau = 200$, 400 and 800. The maximum drag reduction at $Re_\tau = 200$ is found as 50% with forcing parameters $\omega^+ = 0.02$ and $\kappa_x^+ = 0.008$. The figure shows that the drag reduction achieved is reduced at $Re_\tau = 400$ and 800, and the drag increase is also lower at the higher Reynolds numbers. This can be considered as the idea that the overall change in the drag is reduced when the Reynolds number is increased. At $Re_\tau = 400$ the maximum value of $\mathcal{DR}$ drops to 44% with the same control parameters as for $Re_\tau = 200$, and further reduces at $Re_\tau = 800$.

With forcing parameters close to that of maximum drag reduction, the change is large and negative with a reduction of up to 12%, which relates to a reduction in the maximum $\mathcal{DR}$ achieved. This clearly shows a significant Re number effect at the optimal control parameters. Using parameters away from the optimal values gives a relatively small $\Delta\mathcal{DR}$ suggesting that, for example, in the wall oscillation case the larger values of ω^+ may give a more favourable scaling as the Reynolds number is increased. In the region of drag

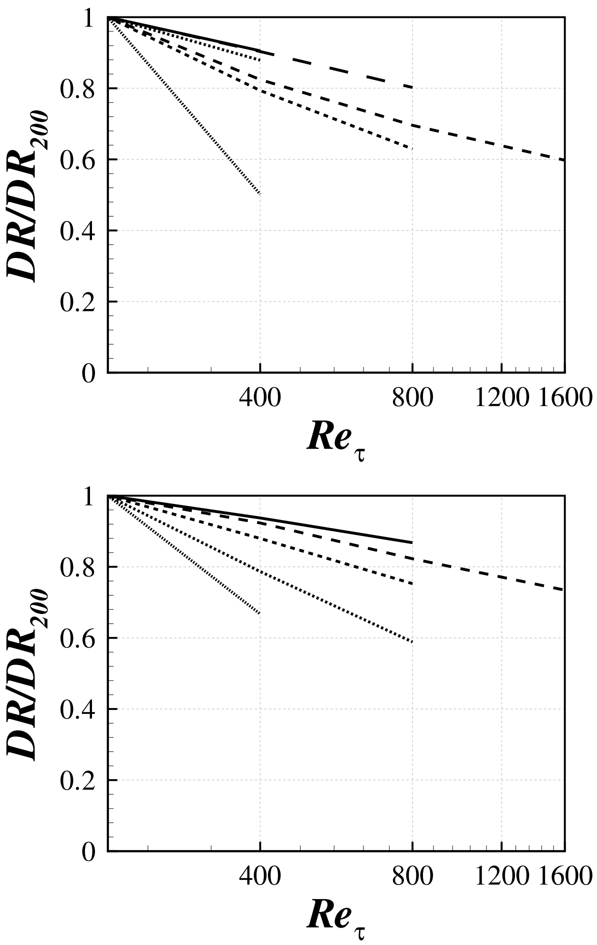

Figure 5: Change in drag reduction with Re_τ scaled by the results from the $Re_\tau = 200$ case. Results are shown for wall oscillation (a) and the stationary wave (b). A longer dash length corresponds to a larger forcing parameter; ω^+ for wall oscillation and κ_x^+ for the stationary wave.

increase, the magnitude of the drag increase is also smaller at the higher Reynolds number.

Figure 4 shows the initial response of the skin-friction to the wall oscillation, normalised by the skin friction from the no control case, $C_{f,0}$. The C_f is much lower at small Re numbers, demonstrating the Re number effect. The level of oscillation in C_f is seen to increase as the Reynolds number is increased. This suggest that the oscillation in the drag reduction does not scale with wall units, and therefore deteriorates the drag achieved rapidly as Re increases, at the optimal parameters. Another interesting point from this figure is that the rate of the initial decay in C_f is very similar at all Reynolds numbers. However this decay is sustained for longer at the lower values of Re.

Re Number Scaling

The drag reduction is scaled by the $Re_\tau = 200$ case and plotted against Reynolds number in Figure 5. Figure 5a shows results from the wall oscillation, with large difference of scaling for this case alone. It was suggested by Ricco and Quadrio (2008) that a stronger effect of Reynolds number occurs for smaller ω^+ (large T^+). This implies that the scaling does not simply become stronger with reduced ω^+ in the whole domain. The results from the stationary wave simulations in Figure 5b also show an increase in Reynolds scaling as κ_x^+ becomes smaller. This is likely due to the limit on the minimum value of κ_x^+ studied, and is expected to behave similarly to that of wall oscillation. Figure 5 highlights the difference in scalings dependent on the forcing parameters chosen. The scaling is not necessarily limited to the range shown in this figure. Instead, it is possible that the scalings have larger variation than presented.

ω^+	0.03	0.06†	0.12
$DR \sim$	$Re_\tau^{-0.31}$	$Re_\tau^{-0.26}$	$Re_\tau^{-0.14}$

Table 2: Wall oscillation.

κ_x^+	0.004	0.006†	0.008‡
$DR \sim$	$Re_\tau^{-0.38}$	$Re_\tau^{-0.18}$	$Re_\tau^{-0.13}$

Table 3: Stationary wave.

A scaling in the form $Re_\tau^{-\alpha}$ is calculated for wall oscillation and stationary wave cases. A large value of α corresponds to a large reduction in $\mathcal{DR}$ as the Reynolds number increases and can therefore be interpreted as an unfavourable scaling. The calculated scalings for wall oscillation control are shown in Table 2, and emphasise the fact that the scaling is much worse at the optimal value of $\omega^+ = 0.06$. Table 3 shows the possible Reynolds number scalings for the stationary wave at different κ_x^+ values. Similarly to the wall oscillation case, the $\mathcal{DR}$ for the stationary wave case is also seen to be affected more by the Reynolds number at lower values of κ_x, where there are large values of α in the scaling. This illustrates how the optimal value of κ_x^+ is increasing with increased Re. The scaling around the region of optimal $\mathcal{DR}$ for the stationary wave is better than for the wall oscillation hinting that, at higher Reynolds number, the stationary wave may remain as a more advantageous control method. However, this may be an artefact of the parameters studied.

The main impact of this is that, although the $\mathcal{DR}$ is reducing as the Reynolds number is increased, and the scaling is strong at the optimal control parameters, by adjusting the control parameters correctly, the scaling with Reynolds number is improved. This means that, at a higher value of Re_τ, using the parameters which were not optimal at low Reynolds number gives a more favourable drag reduction. In the wall oscillation and stationary wave case, lower values of ω^+ and κ_x^+ have higher α values, hence the drag reduction deteriorates more rapidly as the Reynolds number is increased.

Flow Structures

In order to better understand the Reynolds number effect, the flow physics must be considered. Low speed streaks and corresponding flow structures are shown in Figures 6 and 7. Low speed streaks for the stationary wave case is shown in Figure 8.

CONCLUSION

The maximum drag reduction caused by streamwise travelling waves of spanwise velocity reduces as the Reynolds number is increased. The drag reduction deteriorates rapidly at the optimal locations from lower Reynolds number. It is found that the scaling of the drag reduction is not universal. The main implication of this work is to highlight the change

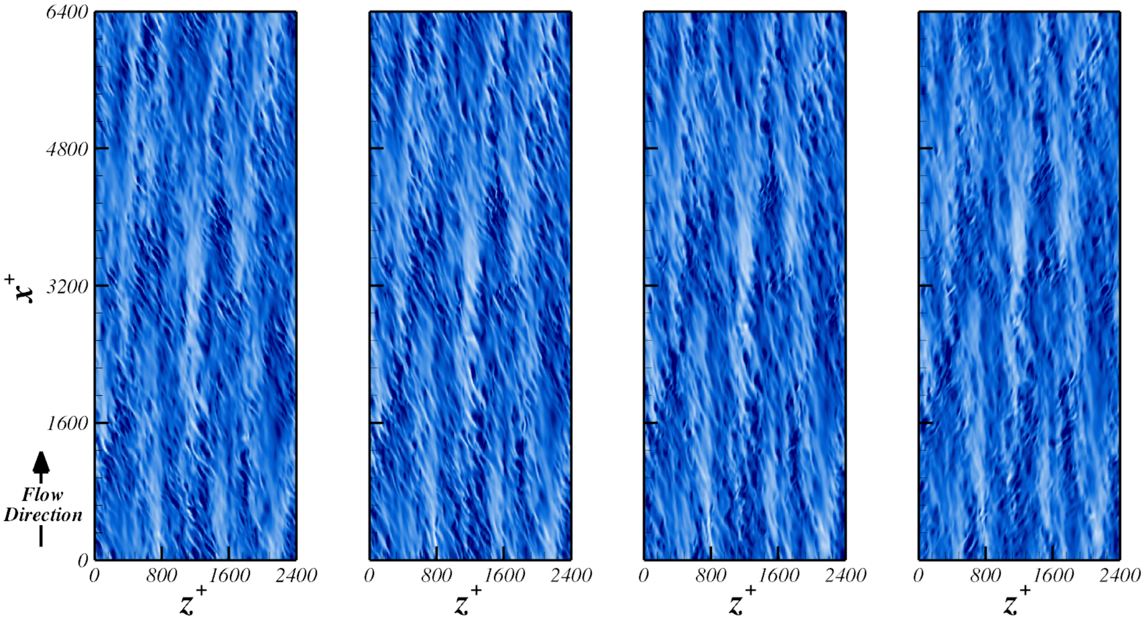

Figure 6: Low-speed streaks at $y^+ = 10$ for wall oscillation case $(\omega^+ = 0.06, T^+ = 100)$ for $Re_\tau = 400$. (a) $\phi = 0$, (b) $\phi = \frac{\pi}{4}$, (c) $\phi = \frac{\pi}{2}$, and (d) $\phi = \frac{3\pi}{4}$.

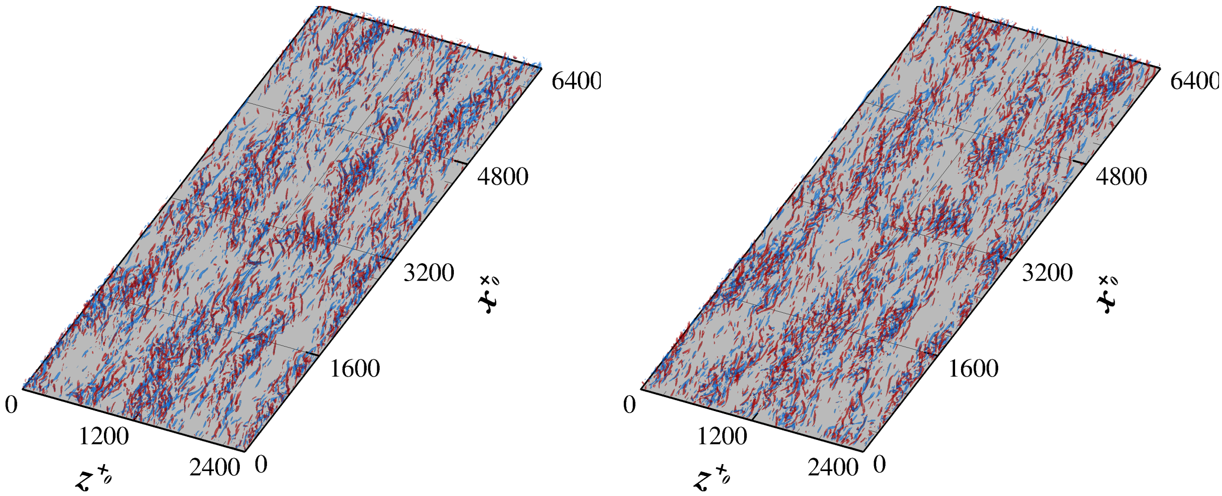

Figure 7: Flow structures (λ_2) for wall oscillation case $(\omega^+ = 0.06, T^+ = 100)$ for $Re_\tau = 400$. (a) $\phi = \frac{\pi}{4}$, and (b) $\phi = \frac{3\pi}{4}$.

in optimal control parameters as the Reynolds number is increased. The scaling with Re is seen to be non-trivial and this means that approximation of the maximum drag reduction achievable at high Reynolds numbers is difficult.

ACKNOWLEDGEMENTS

This work was supported by the EPSRC, Airbus Operations Ltd and EADS UK Ltd (EP/G060215/1). This work has also received support from European commission FP7 projects AirPROM (Grant Agreement FP7 270194, www.airprom.eu), and EPSRC UK Turbulence Consortium (EP/G069581/1). This work made use of the facilities of HECToR, the UK's national high-performance computing service, which is provided by UoE HPCx Ltd at the University of Edinburgh, Cray Inc and NAG Ltd, and funded by the Office of Science and Technology through EPSRC's High End Computing Programme.

REFERENCES

*

References

H. Bieler, A. Abbas, J.-Y. Chiaramonte, and D. Sawyers. Flow control for aircraft performance enhancements - Overview of Airbus - University cooperation. AIAA Paper 2006-3692, 2006.

Y. Chang, S. S. Collis, and S. Ramakrishnan. Viscous effects

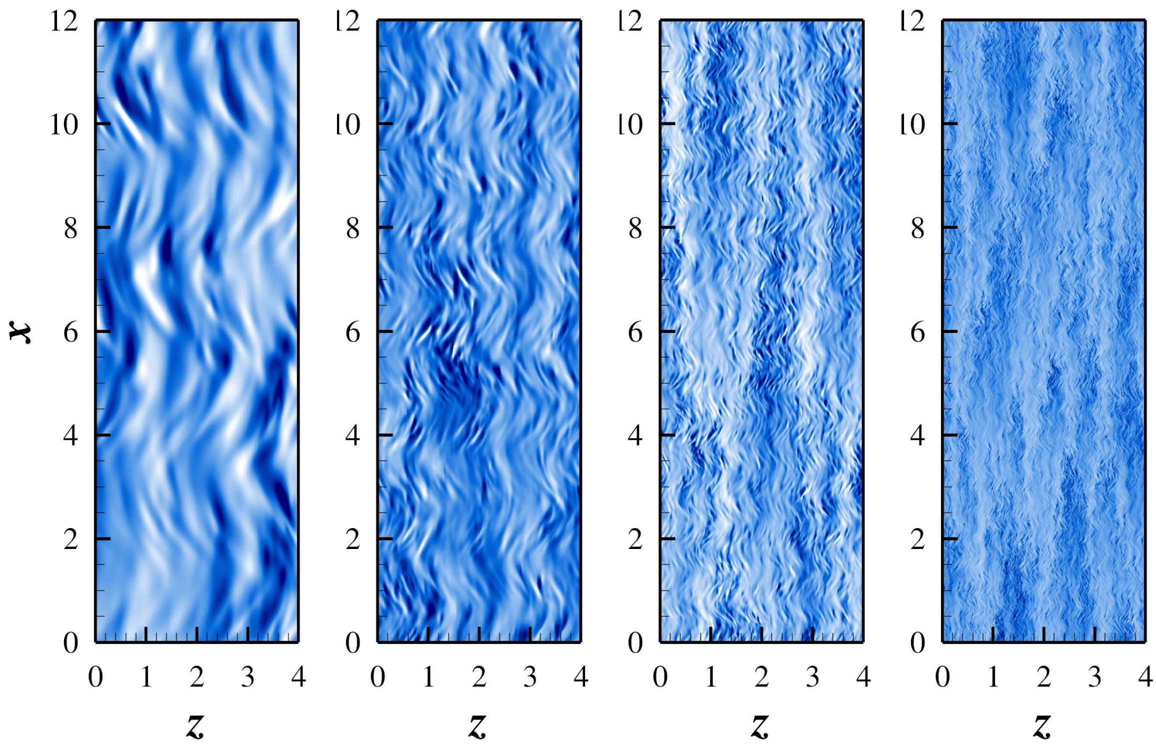

Figure 8: Low-speed streaks at $y^+ = 10$ for stationary wave case ($\kappa_x^+ = 0.008$). (a) $Re_\tau = 200$, (b) $Re_\tau = 400$, (c) $Re_\tau = 800$, and (d) $Re_\tau = 1600$.

in control of near-wall turbulence. *Physics of Fluids*, 14 (11):4069–4080, 2002.

Y. M. Chung and T. Talha. Effectiveness of active flow control for turbulent skin friction drag reduction. *Physics of Fluids*, 23(2):025102, 2011.

E. Hurst and Y. M. Chung. The Reynolds number effect of turbulent drag reduction. In *9th European Fluid Mechanics Conference*, 9-13 September, Rome, Italy, 2012a.

E. Hurst and Y. M. Chung. Turbulent drag reduction by spanwise wall oscillation: The Reynolds number effect. In *Joint ERCOFTAC/PLASMAERO Workshop*, 10-12 December, Toulouse, France, 2012b.

K. Iwamoto, Y. Suzuki, and N. Kasagi. Reynolds number effect on wall turbulence: Toward effective feedback control. *International Journal of Heat and Fluid Flow*, 23 (5):678–689, 2002.

W. J. Jung, N. Mangiavacchi, and R. Akhavan. Suppression of turbulence in wall-bounded flows by high-frequency spanwise oscillations. *Physics of Fluids A*, 4(8):1605–1607, 1992.

G. E. Karniadakis and K.-S. Choi. Mechanisms on transverse motions in turbulent wall flows. *Annual Review of Fluid Mechanics*, 35:45–62, 2003.

K. Kim, S.-J. Baek, and H. J. Sung. An implicit velocity decoupling procedure for the incompressible Navier-Stokes equations. *International Journal for Numerical Methods in Fluids*, 38(2):125–138, 2002.

N. Li and S. Laizet. 2DECOMP and FFT - a highly scalable 2d decomposition library and FFT interface. In *Cray User Group 2010 Conference*, 2010.

M. Quadrio and D. Gatti. What happens to turbulent drag reduction at higher re. In *9th European Fluid Mechanics Conference*, 9-13 September, Rome, Italy, 2012.

M. Quadrio and P. Ricco. Critical assessment of turbulent drag reduction through spanwise wall oscillations. *Journal of Fluid Mechanics*, 521:251–271, 2004.

M. Quadrio, P. Ricco, and C. Viotti. Streamwise-travelling waves of spanwise wall velocity for turbulent drag reduction. *Journal of Fluid Mechanics*, 627:161–178, 2009.

P. Ricco and M. Quadrio. Wall-oscillation conditions for drag reduction in turbulent channel flow. *International Journal of Heat and Fluid Flow*, 29(4):891–902, 2008.

T. Talha. *A numerical investigation of three-dimensional unsteady turbulent channel flow subjected to temporal acceleration.* PhD thesis, School of Engineering, University of Warwick, UK, March 2012.

E. Touber and M. A. Leschziner. Near-wall streak modification by spanwise oscillatory wall motion and drag-reduction mechanisms. *Journal of Fluid Mechanics*, 693: 150–200, 2012.

C. Viotti, M. Quadrio, and P. Luchini. Streamwise oscillation of spanwise velocity at the wall of a channel for turbulent drag reduction. *Physics of Fluids*, 21(11):115109, 2009.